WATER RESEARCH 68 (2015) 24–33

Available online at www.sciencedirect.com

ScienceDirect

journal homepage: www.elsevier.com/locate/watres

Transport, retention, and size perturbation of graphene oxide in saturated porous media: Effects of input concentration and grain size

Yuanyuan Sun [a,b], Bin Gao [b,*], Scott A. Bradford [c], Lei Wu [b], Hao Chen [b], Xiaoqing Shi [a], Jichun Wu [a,*]

[a] State Key Laboratory of Pollution Control and Resource Reuse, Key Laboratory of Surficial Geochemisty, Ministry of Education, School of Earth Sciences and Engineering, Hydrosciences Department, Nanjing University, Nanjing 210093, China

[b] Department of Agricultural and Biological Engineering, University of Florida, Gainesville, FL 32611, USA

[c] USDA-ARS U.S. Salinity Laboratory, Riverside, CA 92507, USA

ARTICLE INFO

Article history:
Received 10 July 2014
Received in revised form
18 September 2014
Accepted 19 September 2014
Available online 2 October 2014

Keywords:
Graphene oxide
Porous media
Deposition mechanisms
Size perturbation
Modeling

ABSTRACT

Accurately predicting the fate and transport of graphene oxide (GO) in porous media is critical to assess its environmental impact. In this work, sand column experiments were conducted to determine the effect of input concentration and grain size on transport, retention, and size perturbation of GO in saturated porous media. The mobility of GO in the sand columns reduced with decreasing grain size and almost all GO were retained in fine sand columns for all of the tested conditions. This result can be explained with colloid filtration and XDLVO theories. Input concentration also influenced the retention and transport of GO in the sand columns because of the 'blocking' mechanism that reduces the particle retention rate. After passing through the column, average GO sizes increased dramatically. In addition, the sizes of GO retained in the sand also increased with travel distance. These results suggested that transport through the porous media induced GO aggregation. A mathematical model based on the advection–dispersion equation coupled with the second-order kinetics to reflect the blocking effect simulated the experimental data well.

© 2014 Elsevier Ltd. All rights reserved.

1. Introduction

Graphene oxide (GO) is a layered carbon-based nanomaterial that contains graphene sheets and oxygen-bearing functional groups (Dreyer et al., 2010). As an emerging class of carbon nanomaterial, GO has received increasing attention in many new fields of application because of its unique structure and exceptional physical and chemical properties (Eda et al., 2008; Chen et al., 2012; Kim et al., 2012; Yang et al., 2013). Given the potential for wide applications and rapid growth in production of this new engineered nanomaterial, it is inevitable that a considerable amount of GO nanoparticles (nanosheets) will be released into the environment, including soil and groundwater systems, during manufacture, transportation, use, and

* *Corresponding authors*. Tel.: +1 352 392 1864x285; fax: +1 352 392 4092.
E-mail addresses: bg55@ufl.edu (B. Gao), jcwu@nju.edu.cn (J. Wu).
http://dx.doi.org/10.1016/j.watres.2014.09.025
0043-1354/© 2014 Elsevier Ltd. All rights reserved.

disposal. Furthermore, recent studies have shown that GO can be toxic toward a variety of organisms including bacteria, animals, and humans (Chang et al., 2011; Wang et al., 2011; Gurunathan et al., 2013). In order to evaluate and determine the environmental impact and potential risk of this new material, an understanding of the transport behavior of GO in porous media is needed.

To date, only few investigations have been directed toward understanding the deposition and transport of GO nanoparticles in porous media (Feriancikova and Xu, 2012; Lanphere et al., 2013; Liu et al., 2013a, 2013b). These studies showed that the mobility of GO nanoparticles is strongly affected by the solution chemistry (e.g., ionic strength), moisture content, and medium surface properties (Feriancikova and Xu, 2012; Lanphere et al., 2013; Liu et al., 2013a, 2013b), which are among the most common environmental conditions that have large influences on the fate and transport of other engineered nanoparticles (Tian et al., 2011, 2012; Liang et al., 2013). In addition, findings from these studies also suggested that current theories and models of colloid (nanoparticle) deposition and transport in porous media can be applied to describe the transport behaviors of GO particles with reasonable accuracies (Feriancikova and Xu, 2012; Lanphere et al., 2013; Liu et al., 2013a, 2013b). Nevertheless, transport and retention processes for GO in porous media are far from fully understood.

Several studies have demonstrated that both particle input concentration and porous medium grain size can strongly affect the deposition and transport of colloidal and nanosized particles in porous media under various conditions (Bradford and Bettahar, 2006; Bradford et al., 2009; Wang et al., 2012a; Liang et al., 2013). Wang et al. (2012a) investigated the effect of input concentration on the retention and transport of silica nanoparticles in porous media and showed that a lower particle number concentration can lead to higher relative retention and less surface coverage. Similarly, Kasel et al. (2013) and Liang et al. (2013) found that that the mobility of functionalized multi-walled carbon nanotubes and silver nanoparticles in porous media increased at higher input concentrations. These effects of input concentration on nanoparticles retention and mobility have typically been attributed to blocking or filling of a limited number of retention sites (Johnson and Elimelech, 1995; Camesano and Logan, 1998; Bradford and Bettahar, 2006). The porous medium grain size has also been found to play an important role in controlling the retention and transport of nanoparticles (Bradford and Bettahar, 2006; Li et al., 2008; Liang et al., 2013). Filtration theory predicts that the nanoparticle mass transfer rate to collector surfaces increases with a decrease in the grain size (Yao et al., 1971; Tufenkji and Elimelech, 2004). The maximum solid phase concentration of retained nanoparticles has also been observed to increase with a decrease in grain size (Li et al., 2008; Liang et al., 2013). Both of these factors indicate that nanoparticle retention is expected to increase in finer grained porous media. Conversely, Tian et al. (2011) found that grain size had little effect on the transport of surfactant-dispersed single-walled carbon nanotubes in saturated porous media. The influence of particle input concentration and porous medium grain size on the transport of GO nanoparticles, which have unique structure and surface properties, still have not yet been reported.

A number of publications have demonstrated that the size distribution of nanoparticle suspensions can change during transport (Solovitch et al., 2010; Chen et al., 2011; Jiang et al., 2012; Wang et al., 2012b, 2012c). Jiang et al. (2012) found that ZnO nanoparticles aggregated during transport, and that the retained aggregate size decreased with transport distance. Wang et al. (2012c) and Solovitch et al. (2010) reported that the average size of TiO_2 nanoparticles increased dramatically after passing through sand columns. Conversely, Chen et al. (2011) and Wang et al. (2012b) found that the size of TiO_2 and Alizarin red S labeled hydroxyapatite nanoparticles, respectively, decreased after transport through sand. Differences in the size distribution of nanoparticles with transport have been associated with non-exponential distributions of retained nanoparticles that are not consistent with filtration theory predictions (Chen et al., 2011; Jiang et al., 2012; Wang et al., 2012b). Previous research has not examined the effects of changes in the graphene oxide size distribution during transport, or determined how this influences the retention profile shape. It is likely that such changes in the retention profile shape will also depend on the input concentration level and the grain size (Kasel et al., 2013; Liang et al., 2013).

The overarching objective of this work was to determine the mechanisms governing GO transport in saturated porous media under different particle input concentration and grain size conditions. Laboratory columns packed with quartz sand of three grain sizes (0.1–0.2 mm, 0.5–0.6, and 0.85–1.0 mm) were used as experimental porous media. Dispersed GO of three concentrations (5, 10, and 25 mg/L) were applied to the columns for breakthrough and retention analysis. The specific objectives were to: (1) determine the effect of particle input concentration and grain size on GO retention and transport, (2) compare the size distribution of GO in influent, effluent and sand media, (3) understand the governing GO retention mechanisms, and (4) model the transport and retention of GO in saturated porous media.

2. Materials and methods

2.1. GO

Single layer GO (ACS Material, Medford, MA), prepared by the modified hummer's method (according to the manufacture), was used as received from the manufacturer. The physical dimensions of GO were determined in a previous study with an atomic force microscope (AFM) and the results indicated that the average thickness and the average square root of the area of the GO are 0.92 ± 0.13 nm and 582 ± 111.2 nm, respectively (Wu et al., 2013).

For stock suspensions preparation, 50 mg of GO were added into 500 mL deionized (DI) water and the mixture was then sonicated for 2 h with a Misonix S3000 ultrasonicator (QSonica, Newtown, CT) for thorough dispersion. Prior to each experiment, the stock solution was diluted to a desired GO concentration and ionic strength (20 mM NaCl) with DI water and a 100 mM NaCl solution. The solution ionic strength was selected based on the findings of our previous

study that GO particles are very stable with low NaCl concentrations (≤30 mM) (Wu et al., 2013). Three input concentration levels (C_o) of 5, 10, or 25 mg/L were employed in the transport experiments. The pH values of the GO suspensions were 4.9–5.4.

Concentrations of the GO suspensions were monitored with an Evolution 60 UV–Vis Spectrophotometer (Thermo Scientific, Waltham, MA) at a wavelength of 230 nm followed the method of Liu et al. (2013a). The hydrodynamic diameter of the GO was measured by a ZetaSizer (Malvern Instruments, Worcestershire, U.K.) with a He–Ne laser (633 nm). The electrophoretic mobility of the GO was determined using a ZetaPlus (Brookhaven Instrument Co., Holtsville, NY). Stability of the GO suspensions was also determined by monitoring the light absorption and hydrodynamic diameter of the GO over time for 8 h and the results indicated that the GO suspensions were stable under the tested experimental conditions (Figure S1, Supporting Information).

2.2. Porous media

Quartz sand (Standard Sand & Silica Co.) was used in this study and was sieved into three different size ranges: fine (0.1–0.2 mm), medium (0.5–0.6 mm), and coarse (0.85–1.0 mm). The sand was washed sequentially by tap water, 10% nitric acid (v:v) and deionized water to remove metal oxides and other impurities following the procedures of Tian et al. (2010). The zeta potential of the sand was measured following the method developed by Johnson et al. (1996).

2.3. GO transport and retention

GO transport experiments were performed in acrylic columns (2.5 cm inner diameter, 16.7 cm length) that were wet-packed with the sands of different sizes (i.e., fine, medium, or coarse). Stainless steel membranes with 50 μm pores (Spectra/Mesh, Spectrum Laboratories, Inc.) were used at both inlet (bottom) and outlet (top) to seal the column and to distribute the flow. Solutions were pumped upward through the column at a constant rate of 1 mL/min (Darcy velocity of 0.2 cm/min) using a peristaltic pump (Masterflex L/S, Cole Parmer Instrument, Vernon Hills, IL).

The packed sand column was first flushed with 4 pore volumes (PVs) of DI water and then 4 PVs of electrolyte solution (20 mM NaCl). A breakthrough experiment was then initiated by injecting a 4 PV pulse of the selected GO suspension (different input concentrations of 5, 10, or 25 mg/L), followed by flushing with 3 PVs of the 20 mM NaCl electrolyte solution. A fraction collector (IS-95 Interval Sampler, Spectrum Chromatography, Houston, TX) was used to collect the effluent samples from the column outlet. The concentration and hydrodynamic diameter of GO in the effluent were measured immediately after sample collection with the methods mentioned previously.

The spatial distributions of retained GO in the sand columns were determined right after the breakthrough experiment. The quartz sand in each column was carefully excavated in ~2 cm increments and transferred into 50 mL vials. The GO particles were detached from the surface of the quartz sand by adding about 20 mL of DI water into the vials and the mixtures were gently shaken for 1 h. Previous studies have shown that DI water can effectively remobilize GO particles retained on sand surfaces (in the secondary minima) (Lanphere et al., 2013). The supernatant was taken immediately to determine the concentrations and the hydrodynamic diameters of the remobilized GO particles. The amount of the sand in each vial was determined after drying in an oven for ≥12 h at a temperature of 60 °C.

2.4. Modeling GO transport and retention

The following mass balance equations were employed to describe the transport and retention of GO in saturated porous media (Bradford et al., 2002):

$$\frac{\partial(\theta C)}{\partial t} = \frac{\partial}{\partial Z}\left(\theta D \frac{\partial C}{\partial Z}\right) - \frac{\partial(qC)}{\partial Z} - \frac{\partial(\rho_b S)}{\partial t} \quad (1)$$

$$\frac{\partial(\rho_b S)}{\partial t} = \theta \psi k C \quad (2)$$

where θ is the volumetric water content [-], C is the aqueous phase GO concentration [N L^{-3}, N and L denote the number of GO and units of length, respectively], t is time [T, T denotes time units], z is the distance from the column inlet [L], D is the hydrodynamic dispersion coefficient[L^2 T^{-1}], q is the Darcy water flux [L T^{-1}], ψ is a dimensionless function to account for site "blocking" [-], k is the "clean-bed", first-order retention coefficient [T^{-1}], ρ_b is the soil bulk density [M L^{-3}, M denote units of mass], and S is the solid phase GO concentration[N M^{-1}]. The first and second terms on the right hand side of Equation (1) account for dispersive and advective transport of GO in the aqueous phase, whereas the third term is used to describe GO retention on the solid phase. The pore water velocity and dispersivity values in the GO transport simulations were based on values determined from the conservative tracer experiments.

The colloid filtration theory has often been applied to model the retention of engineered nanoparticles in saturated porous media (Tian et al., 2010; Feriancikova and Xu, 2012; Gurunathan et al., 2013). In this case, a constant, first-order rate expression (i.e., ψ equals 1) is used to describe the retention kinetics. A number of studies have demonstrated that nanoparticle retention may also be subject to blocking (Bradford et al., 2002; Bradford and Bettahar, 2006; Chowdhury et al., 2011; Kasel et al., 2013; Liang et al., 2013). The site "blocking" effect was modeled using the Langmuirian approach (i.e., second-order kinetics) (Deshpande and Shonnard, 1999) as:

$$\psi = \left(1 - \frac{S}{S_{max}}\right) \quad (3)$$

where S_{max} is the maximum solid phase concentration of deposited GO [N M^{-1}]. Equation (3) assumes that the retention rate linearly decreases as S approaches S_{max}.

The above model was applied to simulate the experimental breakthrough curves (BTCs) and retention profiles (RPs) by simultaneously inverse fitting of k and S_{max} using the Levenberg–Marquardt nonlinear least squares optimization algorithm in HYDRUS-1D.

3. Results and discussion

3.1. XDLVO energy

The average hydrodynamic diameter of GO particles in 20 mM NaCl solution was determined to be 590 ± 94 nm (Figure S1), which is similar to the AFM result (Wu et al., 2013). The electrophoretic mobility and corresponding zeta-potential values of the GO particles and the three types of quartz sand are shown in Table 1. Under the experimental conditions, the electrophoretic mobility values of the GO and the sand were all negative. The corresponding zeta potentials of the GO and the three types of sand were −39.92 to −25.54 mV. Although the tree types of quartz sand were obtained from the same vendor, their zeta potential values were different, probably because they may contain different type of trace elements (Gotze and Lewis, 1994). XDLVO theory was used to calculate the interaction forces between the GO (nanosheets) and the three types of quartz sand, assuming plate–plate interactions (Feriancikova and Xu, 2012; Wu et al., 2013). The XDLVO forces include van der Waals attraction, electric double layer repulsion, and Lewis acid–base interactions. Details about the XDLVO theory can be found in the Supporting Information (S1).

The interaction between the GO and the three types of sand were calculated to be repulsive. Their XDLVO energy profiles all showed energy barriers higher than 11.4 mJ/m^2 (i.e., 2.76 kT/nm^2) to the primary minimum (Fig. 1). It is almost impossible for GO particles to overcome these energy barriers to attach to the sand surfaces in a primary minimum (Shen et al., 2007). However, the XDLVO curves showed the presence of a secondary minimum of -6.77×10^{-4} mJ/m^2 (i.e., -1.64×10^{-4} kT/nm^2), -6.34×10^{-4} mJ/m^2 (i.e., -1.54×10^{-4} kT/nm^2), and -7.34×10^{-4} mJ/m^2 (i.e., -1.78×10^{-4} kT/nm^2) for GO with coarse, medium, and fine sand, respectively. When these values are multiplied by the average cross-sectional area of the GO particles (338,724 nm^2, AFM result (Wu et al., 2013)) then the average depth of the secondary minimum becomes very significant (−49.5 kT). This observation suggests that GO particles may interact with the three types of sand in a secondary minimum. Similar interaction energy profiles for GO particles and quartz sand in electrolyte solutions have been reported in the literature (Feriancikova and Xu, 2012; Liu et al., 2013a).

3.2. GO transport and retention

Observed and simulated BTCs for GO in the saturated sand columns for various grain sizes and input concentration levels are presented in Fig. 2a–c. The data is plotted as normalized effluent concentration (C/C_o) as a function of pore volumes passed through the column. The corresponding RPs for GO in the sand are given in Fig. 2d–f. The RPs are plotted as the normalized solid phase concentration (S/C_o) against the distance from the column inlet (Fig. 2d–f). The simulations were obtained from the solution of Equations (1)–(3). Mass balance information (effluent, sand, and total) for these experiments is provided in Table 2. A summary of the fitted model parameters is given in Table 3, as well as the Pearson's correlation coefficient for the goodness of model fit (R^2).

Colloid filtration theory (Yao et al., 1971) predicts BTCs that are symmetric and RPs that are exponential with depth. Conversely, the BTCs for GO tended to be asymmetric, with values of C/C_o increasing with continued GO injection. Asymmetric breakthrough behavior has been observed in previous studies of colloid and nanoparticle transport in saturated porous media (Bradford et al., 2002; Bradford and Bettahar, 2006; Chowdhury et al., 2011; Kasel et al., 2013; Liang et al., 2013). Findings from these studies suggest that this time-dependent retention process cannot be simply described as a constant rate, first-order deposition coefficient. Instead, the kinetics of particle retention on grain surfaces will decrease over time as the attachment sites are blocked or filled by previously retained particles (Bradford et al., 2002; Bradford and Bettahar, 2006). Similarly, the shape of the GO RPs in this work was inconsistent with the predictions of clean-bed filtration theory. Blocking will also influence the shape of the RPs. In particular, RPs will transition from exponential to uniform with depth as the S approaches S_{max}. With best-fit parameters, the blocking model matched the experimental BTCs and RPs very well (Fig. 2, Table 3).

Mass balance calculations indicated that the total column mass balance ranged from 96.2% to 113.2% (Table 2), providing a high degree of confidence in our experimental procedures. The mass balance results also confirm that GO retention on the sand surface was strongly influenced by the secondary minima because almost all of the previously retained GO particles were released from the sand after washing with DI water (Hahn and O'Melia, 2004). When the solution chemistry changed from 20 mM NaCl to DI water, the secondary minima disappears because of an increase in double layer thickness. XDLVO profiles of the interactions between GO and the three types of sand in DI water can be found in Figure S2 of the Supporting Information.

3.3. Grain size

Fig. 2 indicates that the sand grain size had a strong influence on the amount of GO transport and retention. In comparison with the coarse and medium sand, the fine sand had the highest removal of GO particles under the tested conditions. In fact, nearly no breakthrough of GO in the fine sand columns was observed for all three input concentrations (Fig. 2c). Mass balance calculations showed that less than 1% of GO were recovered in the effluents of the fine sand (Table 2). The mobility of GO in the coarse and medium sand columns were higher with recovery rates of 26.6%–56.9% and 16.4%–33.2% (Table 2), respectively, depending on C_o. Retention of GO at a given C_o tended to increase with decreasing sand size (e.g., fine > medium > coarse). Several previous studies have also

Table 1 – Basic surface properties of GO and sand medium.

	Electrophoretic mobility ($\times 10^{-8}$ m^2/V)	Zeta-potential (mV)
GO	−2.27 ± 0.12	−30.73 ± 1.58
Sand (coarse)	−2.48 ± 0.16	−32.56 ± 2.14
Sand (medium)	−2.95 ± 0.20	−39.92 ± 2.76
Sand (fine)	−1.89 ± 0.15	−25.54 ± 2.05

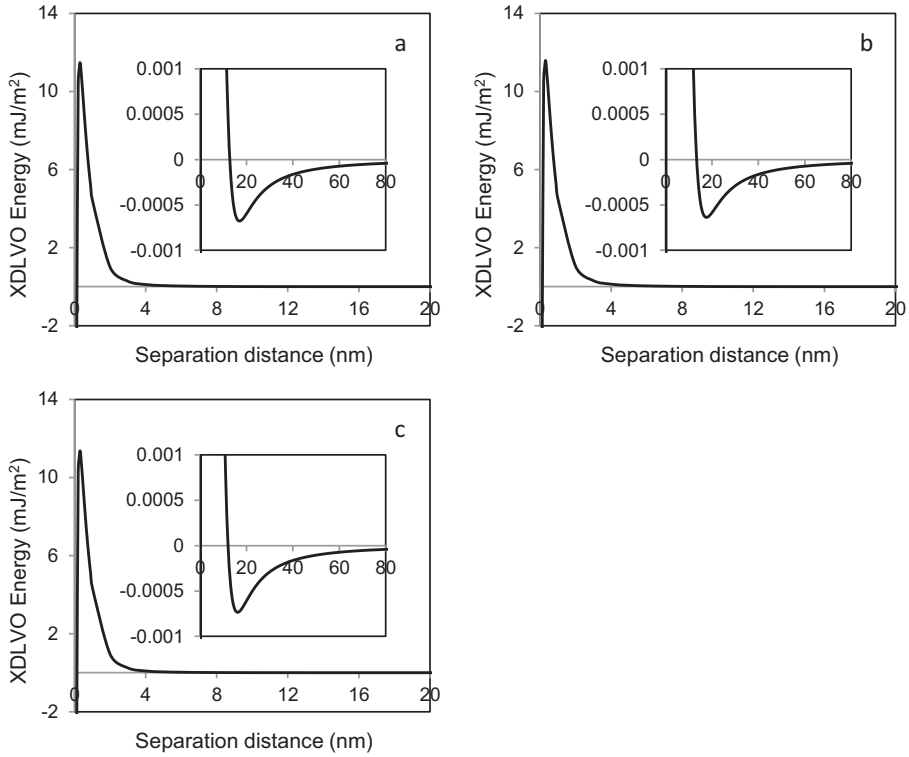

Fig. 1 – XDLVO energy between GO particles and coarse (a), medium (b), or fine (c) sand in 20 mM NaCl solution.

observed that the retention of other engineering nanoparticles in saturated porous media increased when the porous medium grain size decreased (Kasel et al., 2013; Liang et al., 2013). Kasel et al. (2013) and Liang et al. (2013) have attributed this effect to an increasing rate of mass transfer to the collector surface as the grain size decreases. This trend is predicted by colloid filtration (Yao et al., 1971; Tufenkji and Elimelech, 2004). Furthermore, the XDLVO energy profiles

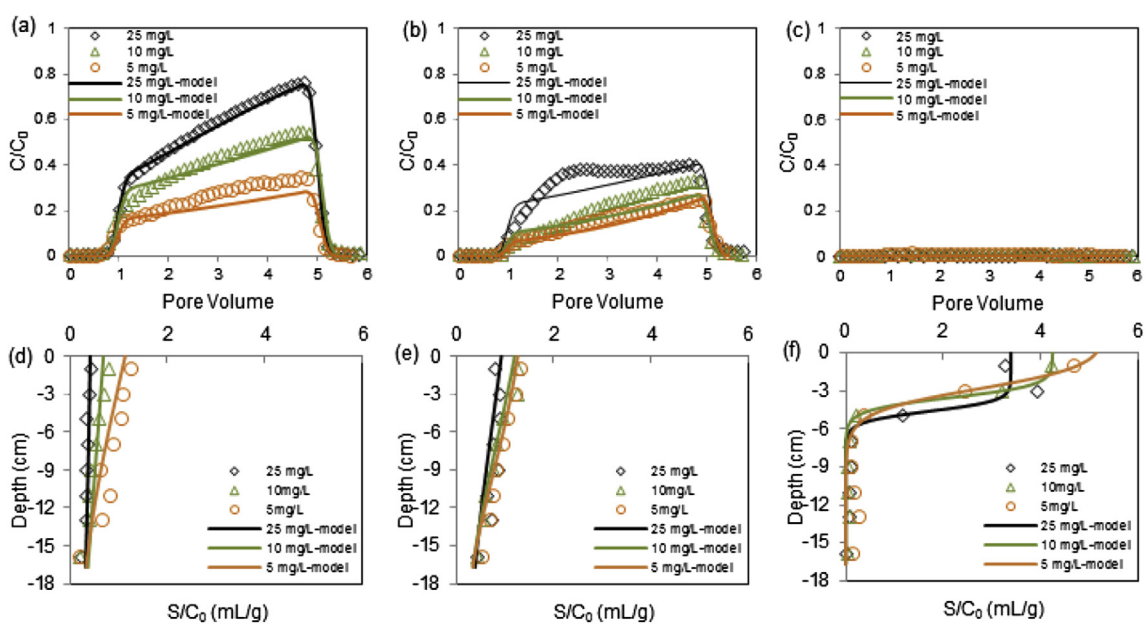

Fig. 2 – Observed and simulated (using best-fit deposition parameters) breakthrough curves (a–c) and retention profiles (d–f) of GO of different input concentrations in coarse (a, d), medium (b, e), and fine (c, f) sand columns. Symbols are experimental data and lines are model results.

Table 2 – Summary of experimental conditions and mass balance information.[a]

Sand size	Input concentration (Mg/L)	Porosity	Pore velocity (cm/min)	Disp.(cm)	M_E	M_R	M_T
Coarse	25	0.39	0.52	0.1195	56.9%	39.7%	96.6%
Coarse	10	0.39	0.52	0.1195	41.5%	54.7%	96.2%
Coarse	5	0.39	0.52	0.1195	26.6%	86.6%	113.2%
Medium	25	0.41	0.51	0.1038	33.2%	78.1%	111.3%
Medium	10	0.41	0.51	0.1038	20.3%	86.5%	106.8%
Medium	5	0.41	0.51	0.1038	16.4%	94.2%	110.6%
Fine	25	0.39	0.52	0.0504	0.22%	103.3%	103.5%
Fine	10	0.39	0.52	0.0504	0.57%	97.2%	97.8%
Fine	5	0.39	0.52	0.0504	0.57%	102.0%	102.6%

[a] Disp. is the longitudinal dispersivity determined on basis of the conservative tracer study, and M_E, M_R, and M_T are mass percentages recovered from effluent, sand and total, respectively.

(Fig. 1) show that the depths of the secondary minimum wells for the three types of sand were similar, suggesting that they should have similar attachment efficiencies (Hahn et al., 2004). Thus the overall removal rate of the GO by sand should increase with decreasing grain size.

The best-fit values of k ranged from 0.03 to 0.06, 0.05–0.09, and 0.61–1.39 min^{-1} for GO retention on coarse, medium, and fine sand grains, respectively (Table 3). As discussed above, this result is consistent with the predictions of colloid filtration theory and XDLVO theory that finer sand should have higher GO removal efficiencies. The best-fit values of S_{max} ranged from 10.5 to 12.3, 7.7–38.9, and 26.7–84.6 μg/g for coarse, medium, and fine sand grains, respectively. For a given C_o the value of S_{max} increased with decreasing sand grain size. This observation suggests that the number of attachment sites for GO retention increases with the surface area of the sand. It also implies that blocking should be more important in coarser textured sand. Indeed, Fig. 2 indicates that blocking effects on the BTCs (asymmetric) and RPs (transitioning from exponential to uniform with depth) are more pronounced in coarser textured sand.

It should be noted that the RPs in the fine sand columns looked similar to an exponential shape. However, the amount of particles retained in the first two layers, which is more than 90% of the total GO mass, was very close to each other (Fig. 2f). In this case, most of the attachment sites in these two layers were occupied by GO particles. This further confirmed that previously retained GO particles can block or fill retention sites on grain surfaces. The high values of k and S_{max} in the fine sand produced more than 99% retention under the tested experimental conditions. This implies that fine sand can potentially be used as a low-cost filter media to remove GO from water. The high recovery of the GO from the sand indicates that the filter sand can be regenerated by simply mixing and rinsing with DI water.

3.4. *Input concentration*

It was hard to determine the effect of input concentration on GO transport in fine sand columns because there was no/little GO breakthrough (Fig. 2c). However, less GO breakthrough occurred with lower input concentration in the coarse and medium sand columns (Fig. 2a and b). Mass balance calculations indicated that the recovery rates of GO in the effluents almost doubled for both coarse (26.6%–56.9%) and medium (16.4%–33.2%) sand when the input concentration increased from 5 to 25 mg/L (Table 2). This concentration dependent transport behavior can be explained by blocking. In particular, attachment sites are filled more rapidly by a higher input concentration. This produces a larger reduction in the retention rate and thereby diminishes retention and increases the potential for GO transport in the sand.

The best-fit values of k and S_{max} for the different experimental systems are presented in Table 3. These values were obtained through inverse modeling without any physical constraints. Filtration theory and XDLVO calculations do not predict a dependence of k and S_{max} on C_o. Interestingly, values of k and S_{max} were found to systematically change with C_o. In particular, the value of S_{max} was found to increase with increasing C_o for most of the cases. It is possible that this trend

Table 3 – Model parameters of GO retention and transport in the sand columns under various experimental conditions.

Sand size	Input concentration (mg/L)	Best-fit parameters			Average S_{max}		
		k (min^{-1})	S_{max} (μg/g)	R^2	k (min^{-1})	S_{max} (μg/g)	R^2
Coarse	25	0.0335	12.32	0.9883	0.0353	11.08	0.9887
Coarse	10	0.0400	10.43	0.9554	0.0390	11.08	0.9551
Coarse	5	0.0579	10.50	0.9663	0.0571	11.08	0.9658
Medium	25	0.0456	38.87	0.9274	0.0608	21.07	0.8200
Medium	10	0.0699	16.66	0.9847	0.0642	21.07	0.9801
Medium	5	0.0866	7.665	0.9911	0.0614	21.07	0.9586
Fine	25	1.388	84.60	0.9881	0.4411	51.22	0.7562
Fine	10	1.128	42.39	0.9995	0.5606	51.22	0.9706
Fine	5	0.610	26.68	0.9945	0.3464	51.22	0.9856

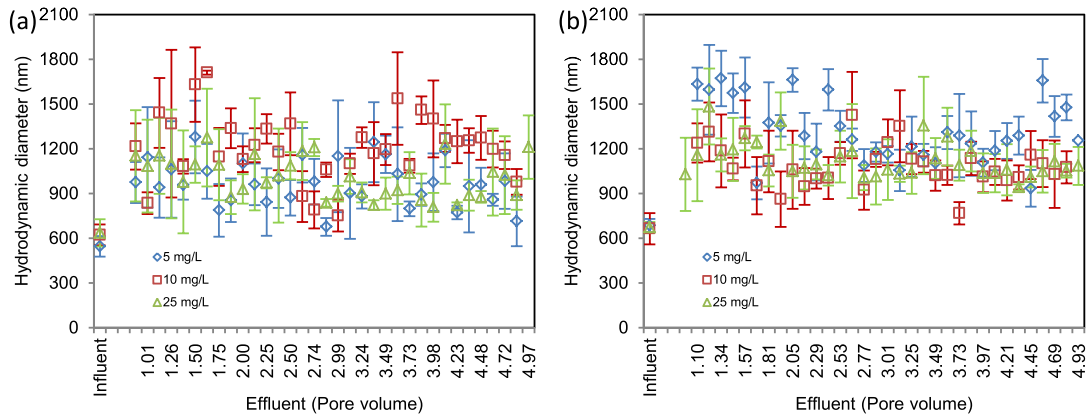

Fig. 3 – Size distributions of GO in influents and effluents of coarse (a) and medium (b) sand columns. Data are expressed as means ± standard deviation ($n = 4$–9).

maybe an artifact of the selected blocking model. For example, the dependence of S_{max} on C_o may be different when using the random sequential adsorption model (Johnson and Elimelech, 1995), which assumes a nonlinear dependency on S during blocking. Additional simulations of the BTC and RP data were conducted when using the average best-fit value of S_{max} (Table 3) for each sand type (from three GO input concentrations). The new model simulations still matched all the experimental BTCs and RPs well with seven out of nine R^2 values larger than 0.95 and the other two larger than 0.75 (Table 3 and Figure S4, Supporting Information). This observation suggests that Equation (3) provided an adequate description of the 'blocking' effect for various C_o values when using average values of S_{max}.

3.5. *GO size distributions*

The size distributions of the GO particles in the influents, effluents, and sand media were monitored by measuring their hydrodynamic diameters. Although the hydrodynamic

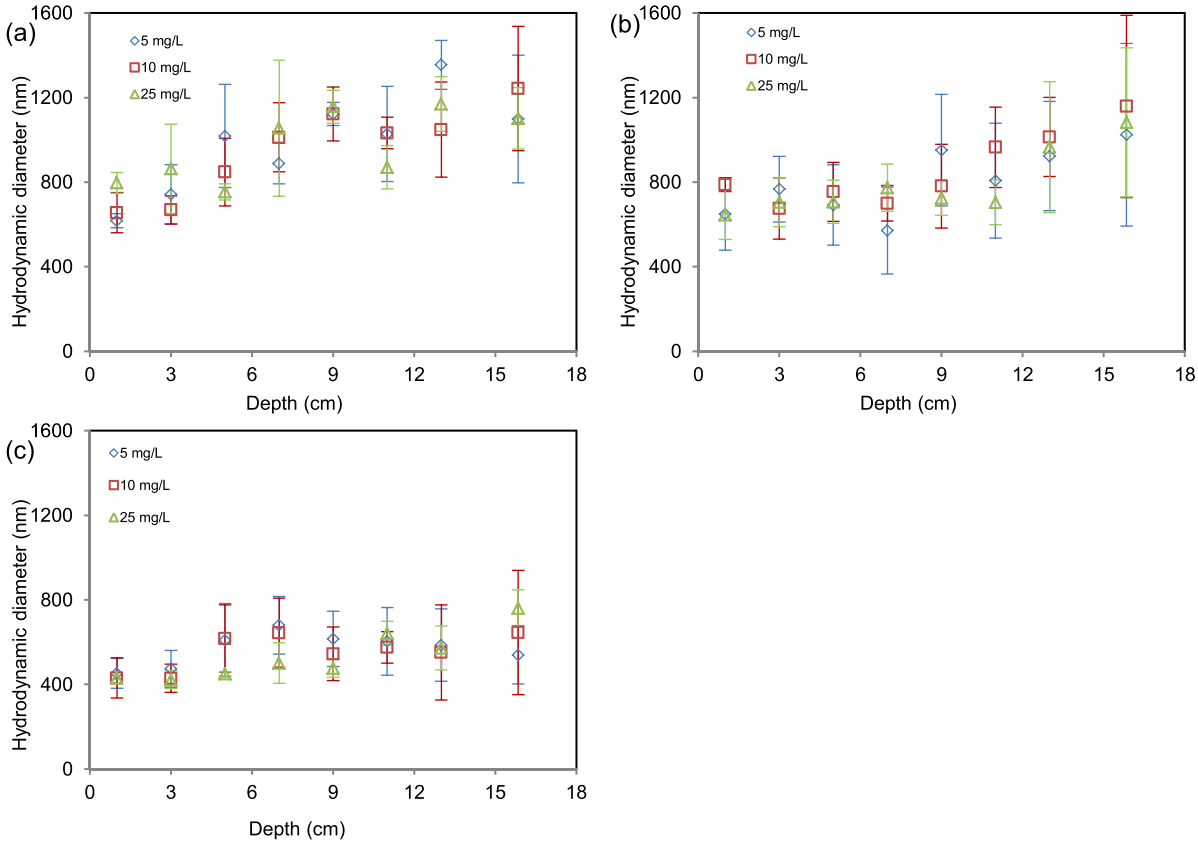

Fig. 4 – Size distribution of retained GO in coarse (a), medium (b) and fine (c) sand columns. Data are expressed as means ± standard deviation ($n = 4$–9).

diameter measurement may not be the most accurate method to determine the actual GO sizes, it can still provide reasonable representations of the size distributions of GO nanosheet, particularly with respect to the trend of GO size perturbations (Chowdhury et al., 2013; Wu et al., 2013).

In this work, the hydrodynamic diameters of GO in the influents remained the same before and after the breakthrough experiment for all the tested conditions, which is consistent with the results of the stability test (Figure S1, supporting information). After passing through the coarse and medium sand column (no/little breakthrough in fine sand), the hydrodynamic diameters of GO in the effluents increased dramatically for all the samples collected at different time intervals (Fig. 3). Because the GO sizes in the effluents at different pore volumes were close to each other for all combinations of input concentrations (i.e., 5, 10, and 25 mg/L) and two sand (i.e., coarse and medium), average hydrodynamic diameters were thus used to compare GO sizes before and after passing through the sand columns. For coarse sand columns, the average size of GO in the influents was 574 ± 82 nm and it increased to 1059 ± 267 nm in the effluents. For the medium sand columns, the average size of GO increased from 678 ± 63 nm to 1176 ± 246 nm after passing through the columns. The size distributions of retained GOs in all the sand columns also showed a trend of increasing particle sizes with travel distance (Fig. 4). The GO size almost remained the same as that of the input in the segment near the column inlet, then increased with increasing transport distance, and finally reached the largest in the segment near the column outlet. Regression analysis showed that there are relatively strong upward trends of the average GO size for each input concentration in all the columns (Figure S3, Supporting Information). Furthermore, the slope and intercept of the regression lines increased with increasing sand grain size.

Previous studies of other engineered nanoparticles, such as TiO_2 nanoparticles, have reported an increase in size after passing through porous media (Solovitch et al., 2010; Chen et al., 2011; Wang et al., 2012c). One potential explanation comes from colloid filtration theory predictions that the contact efficiency increases with decreasing particle size when the suspended particles are smaller than 2 μm (Yao et al., 1971; Tufenkji and Elimelech, 2004). Consequently, smaller particles are expected to have a faster deposition rate than the larger ones (when they are smaller than 2 μm), and the average GO size is therefore expected to increase with distance from the column inlet. This hypothesis implies that the variance of the GO size would decrease with transport distance. Conversely, the error bars on the data presented in Figs. 3 and 4 indicate that the variance of the GO size became larger after passing the column. In addition, this hypothesis also indicates that the retention rate coefficient would be depth-dependent (Yao et al., 1971; Tufenkji and Elimelech, 2004), whereas the RPs in Fig. 2 were well described using Equations (1)–(3).

An alternative hypothesis for an increasing particle size with transport distance is simultaneous particle aggregation and deposition in porous media (Solovitch et al., 2010). Although the GO particles in the influents were stable, their aggregation rate might increase after entering the porous media. In support of this hypothesis, Figs. 3 and 4 indicate that the GO particle size and variance increased when passing through the porous media. Aggregation in porous media may occur by ripening when retained particles act as attachment sites for retention (Tong et al., 2008), but ripening is typically associated with a decreasing breakthrough curve shape with continued particle injection which was not observed in Fig. 2. Alternatively, flow induced aggregation may also occur in porous media when advective transport provides sufficient energy for colliding particles to overcome the energy barrier and aggregate (Chen et al., 2011). Further investigations are needed to better determine and quantify the controlling mechanisms of particle size increase during filtration.

4. Conclusions

This work provides new information on retention and transport of GO particles in saturated porous media by not only evaluating their BTCs and RPs but also monitoring their size perturbations in the influents and effluents, and within the sand columns. The results demonstrated that both input concentration and grain size have impact on the transport and retention of GO in porous media. While the grain size effect on GO deposition on sand surface matched the predictions of the colloid filtration theory and the XDLVO theory, the input concentration effect reflected the site 'blocking' mechanism that is not included in the classic theories. After passing through the columns, the size of the GO particles increased with travel distance. Classic colloid filtration theory could not explain the observed changes in the GO particle size with transport distance. Conversely, results suggestion that transport through the porous media induced GO aggregation. This suggested that, in order to accurately predict the fate and transport of GO particles in porous media, mathematical models should be derived in a mechanistic way to reflect the governing deposition and aggregation mechanisms. Findings from this study also suggested that sandy porous media, particularly fine sand, may be used as filter material to remove GO from water.

Acknowledgment

This work was partially supported the NSFC (41030746 and 41372234) and NSF (CBET-1213333). Y.S. acknowledges the support of the China Research Council Scholarship.

Appendix A. Supplementary data

Supplementary data related to this article can be found at http://dx.doi.org/10.1016/j.watres.2014.09.025.

REFERENCES

Bradford, S.A., Yates, S.R., Bettahar, M., Simunek, J., 2002. Physical factors affecting the transport and fate of colloids in saturated porous media. Water Resour. Res. 38 (12), 1327 doi: 1310.1029/2002WR001340.

Bradford, S.A., Bettahar, M., 2006. Concentration dependent transport of colloids in saturated porous media. J. Contam. Hydrol. 82 (1–2), 99–117.
Bradford, S.A., Kim, H.N., Haznedaroglu, B.Z., Torkzaban, S., Walker, S.L., 2009. Coupled factors influencing concentration-dependent colloid transport and retention in saturated porous Media. Environ. Sci. Technol. 43 (18), 6996–7002.
Camesano, T.A., Logan, B.E., 1998. Influence of fluid velocity and cell concentration on the transport of motile and nonmotile bacteria in porous media. Environ. Sci. Technol. 32 (11), 1699–1708.
Chang, Y.L., Yang, S.T., Liu, J.H., Dong, E., Wang, Y.W., Cao, A.N., Liu, Y.F., Wang, H.F., 2011. In vitro toxicity evaluation of graphene oxide on A549 cells. Toxicol. Lett. 200 (3), 201–210.
Chen, D., Feng, H., Li, J., 2012. Graphene oxide: preparation, functionalization, and electrochemical applications. Chem. Rev. 112 (11), 6027–6053.
Chen, G.X., Liu, X.Y., Su, C.M., 2011. Transport and retention of TiO2 Rutile nanoparticles in saturated porous media under low-ionic-strength conditions: measurements and mechanisms. Langmuir 27 (9), 5393–5402.
Chowdhury, I., Hong, Y., Honda, R.J., Walker, S.L., 2011. Mechanisms of TiO_2 nanoparticle transport in porous media: role of solution chemistry, nanoparticle concentration, and flowrate. J. Colloid Interface Sci. 360 (2), 548–555.
Chowdhury, I., Duch, M.C., Mansukhani, N.D., Hersam, M.C., Bouchard, D., 2013. Colloidal properties and stability of graphene oxide nanomaterials in the aquatic environment. Environ. Sci. Technol. 47 (12), 6288–6296.
Deshpande, P.A., Shonnard, D.R., 1999. Modeling the effects of systematic variation in ionic strength on the attachment kinetics of Pseudomonas fluorescens UPER-1 in saturated sand columns. Water Resour. Res. 35 (5), 1619–1627.
Dreyer, D.R., Park, S., Bielawski, C.W., Ruoff, R.S., 2010. The chemistry of graphene oxide. Chem. Soc. Rev. 39 (1), 228–240.
Eda, G., Fanchini, G., Chhowalla, M., 2008. Large-area ultrathin films of reduced graphene oxide as a transparent and flexible electronic material. Nat. Nanotechnol. 3 (5), 270–274.
Feriancikova, L., Xu, S.P., 2012. Deposition and remobilization of graphene oxide within saturated sand packs. J. Hazard. Mater. 235, 194–200.
Gotze, J., Lewis, R., 1994. Distribution of REE and trace elements in size and mineral fractions of high-purity quartz sands. Chem. Geol. 114 (1–2), 43–57.
Gurunathan, S., Han, J.W., Eppakayala, V., Kim, J.H., 2013. Biocompatibility of microbially reduced graphene oxide in primary mouse embryonic fibroblast cells. Colloids Surfaces B-biointerfaces 105, 58–66.
Hahn, M.W., Abadzic, D., O'Melia, C.R., 2004. Aquasols: on the role of secondary minima. Environ. Sci. Technol. 38 (22), 5915–5924.
Hahn, M.W., O'Melia, C.R., 2004. Deposition and reentrainment of Brownian particles in porous media under unfavorable chemical conditions: some concepts and applications. Environ. Sci. Technol. 38 (1), 210–220.
Jiang, X.J., Tong, M.P., Lu, R.Q., Kim, H., 2012. Transport and deposition of ZnO nanoparticles in saturated porous media. Colloids Surfaces A-physicochem. Eng. Aspects 401, 29–37.
Johnson, P.R., Elimelech, M., 1995. Dynamics of colloid deposition in porous-media – blocking based on random sequential adsorption. Langmuir 11 (3), 801–812.
Johnson, P.R., Sun, N., Elimelech, M., 1996. Colloid transport in geochemically heterogeneous porous media: modeling and measurements. Environ. Sci. Technol. 30 (11), 3284–3293.
Kasel, D., Bradford, S.A., Simunek, J., Heggen, M., Vereecken, H., Klumpp, E., 2013. Transport and retention of multi-walled carbon nanotubes in saturated porous media: effects of input concentration and grain size. Water Res. 47 (2), 933–944.
Kim, J., Cote, L.J., Huang, J., 2012. Two dimensional soft material: new faces of graphene oxide. Accounts Chem. Res. 45 (8), 1356–1364.
Lanphere, J.D., Luth, C.J., Walker, S.L., 2013. Effects of solution chemistry on the transport of graphene oxide in saturated porous Media. Environ. Sci. Technol. 47 (9), 4255–4261.
Li, Y.S., Wang, Y.G., Pennell, K.D., Abriola, L.M., 2008. Investigation of the transport and deposition of fullerene (C60) nanoparticles in quartz sands under varying flow conditions. Environ. Sci. Technol. 42 (19), 7174–7180.
Liang, Y., Bradford, S.A., Simunek, J., Vereecken, H., Klumpp, E., 2013. Sensitivity of the transport and retention of stabilized silver nanoparticles to physicochemical factors. Water Res. 47 (7), 2572–2582.
Liu, L., Gao, B., Wu, L., Morales, V.L., Yang, L.Y., Zhou, Z.H., Wang, H., 2013a. Deposition and transport of graphene oxide in saturated and unsaturated porous media. Chem. Eng. J. 229, 444–449.
Liu, L., Gao, B., Wu, L., Yang, L.Y., Zhou, Z.H., Wang, H., 2013b. Effects of pH and surface metal oxyhydroxides on deposition and transport of carboxyl-functionalized graphene in saturated porous media. J. Nanoparticle Res. 15 (11).
Shen, C.Y., Li, B.G., Huang, Y.F., Jin, Y., 2007. Kinetics of coupled primary- and secondary-minimum deposition of colloids under unfavorable chemical conditions. Environ. Sci. Technol. 41 (20), 6976–6982.
Solovitch, N., Labille, J., Rose, J., Chaurand, P., Borschneck, D., Wiesner, M.R., Bottero, J.Y., 2010. Concurrent aggregation and deposition of TiO_2 nanoparticles in a sandy porous Media. Environ. Sci. Technol. 44 (13), 4897–4902.
Tian, Y., Gao, B., Wu, L., Munoz-Carpena, R., Huang, Q., 2012. Effect of solution chemistry on multi-walled carbon nanotube deposition and mobilization in clean porous media. J. Hazard. Mater. 231, 79–87.
Tian, Y.A., Gao, B., Silvera-Batista, C., Ziegler, K.J., 2010. Transport of engineered nanoparticles in saturated porous media. J. Nanoparticle Res. 12 (7), 2371–2380.
Tian, Y.A., Gao, B., Ziegler, K.J., 2011. High mobility of SDBS-dispersed single-walled carbon nanotubes in saturated and unsaturated porous media. J. Hazard. Mater. 186 (2–3), 1766–1772.
Tong, M.P., Ma, H.L., Johnson, W.P., 2008. Funneling of flow into grain-to-grain contacts drives colloid-colloid aggregation in the presence of an energy barrier. Environ. Sci. Technol. 42 (8), 2826–2832.
Tufenkji, N., Elimelech, M., 2004. Correlation equation for predicting single-collector efficiency in physicochemical filtration in saturated porous media. Environ. Sci. Technol. 38 (2), 529–536.
Wang, C., Bobba, A.D., Attinti, R., Shen, C.Y., Lazouskaya, V., Wang, L.P., Jin, Y., 2012a. Retention and transport of silica nanoparticles in saturated porous media: effect of concentration and particle size. Environ. Sci. Technol. 46 (13), 7151–7158.
Wang, D.J., Bradford, S.A., Harvey, R.W., Gao, B., Cang, L., Zhou, D.M., 2012b. Humic acid facilitates the transport of ARS-labeled hydroxyapatite nanoparticles in iron oxyhydroxide-coated sand. Environ. Sci. Technol. 46 (5), 2738–2745.
Wang, K., Ruan, J., Song, H., Zhang, J.L., Wo, Y., Guo, S.W., Cui, D.X., 2011. Biocompatibility of graphene oxide. Nanoscale Res. Lett. 6.
Wang, Y., Gao, B., Morales, V.L., Tian, Y., Wu, L., Gao, J., Bai, W., Yang, L., 2012c. Transport of titanium dioxide nanoparticles in saturated porous media under various solution chemistry conditions. J. Nanoparticle Res. 14 (9), 1095.

Wu, L., Liu, L., Gao, B., Munoz-Carpena, R., Zhang, M., Chen, H., Zhou, Z., Wang, H., 2013. Aggregation kinetics of graphene oxides in aqueous solutions: experiments, mechanisms, and modeling. Langmuir 29, 15174–15181.

Yang, Z., Yan, H., Yang, H., Li, H., Li, A., Cheng, R., 2013. Flocculation performance and mechanism of graphene oxide for removal of various contaminants from water. Water Res. 47 (9), 3037–3046.

Yao, K.M., Habibian, M.M., Omelia, C.R., 1971. Water and waste water filtration - concepts and applications. Environ. Sci. Technol. 5 (11), 1105–1112.